

Porosity in plasma sprayed alumina coatings.

Authors:

Jan Ilavsky, H. Herman, C.C. Berndt
SUNY at Stony Brook, Stony Brook, NY

A. N. Goland
Brookhaven National Laboratory, Upton, NY

G. G. Long, S. Krueger, A. J. Allen
National Institute of Standards and Technology, Gaithersburg, MA

Keywords: Porosity, Small-Angle Neutron Scattering, Alumina Deposits, MIP, Water Immersion, Pore Sizes

DISCLAIMER

This report was prepared as an account of work sponsored by an agency of the United States Government. Neither the United States Government nor any agency thereof, nor any of their employees, makes any warranty, express or implied, or assumes any legal liability or responsibility for the accuracy, completeness, or usefulness of any information, apparatus, product, or process disclosed, or represents that its use would not infringe privately owned rights. Reference herein to any specific commercial product, process, or service by trade name, trademark, manufacturer, or otherwise does not necessarily constitute or imply its endorsement, recommendation, or favoring by the United States Government or any agency thereof. The views and opinions of authors expressed herein do not necessarily state or reflect those of the United States Government or any agency thereof.

MASTER

DISTRIBUTION OF THIS DOCUMENT IS UNLIMITED

for
RECORDED

MAR 30 1994

OSTI

Abstract

Small-angle neutron scattering (SANS) has been used to study the porosity of plasma sprayed deposits of alumina in the as-sprayed and heat-treated conditions. The SANS results were compared with results from two intrusion techniques; i.e., mercury intrusion porosimetry (MIP) and water immersion techniques. Multiple small-angle neutron scattering yields a volume-weighted effective pore radius (R_{eff}), for pores with sizes between 0.08 and 10 μm , the pore volume in this size region, and from the Porod region, the surface area of pores of all sizes.

Plasma sprayed samples were studied in the as-sprayed condition and following heat treatments at 1300°C and 1500°C for 2 h. Mercury intrusion porosimetry measured most or all of the samples' porosity, i.e., the total connected porosity. Porosity volumes derived from SANS were close to the MIP results for heat treated samples whereas the SANS results for the as-sprayed samples were smaller. This suggests changes in pore size during heat treatment. The measured R_{eff} was about 0.6 to 1.0 μm for all samples except for the sample manufactured from gray alumina and heat treated for 2 h at 1500°C. The R_{eff} of this sample increased to 2.2 μm ; probably due to rapid sintering resulting in redistribution of the pore sizes.

The pore surface areas varied between 1.5 and $7.6 \times 10^4 \text{ cm}^2/\text{cm}^3$ during heat treatment. Original surface areas increased 2 to 3 times during the 1300°C heat treatment and then decreased up to 5 times (from the 1300°C value) after a 1500°C heat treatment. The results of SANS measurements agreed with the processes in the plasma sprayed deposits during heat treatment and with the results of intrusion techniques.

POROSITY IS AN INTRINSIC microstructural characteristic of plasma-sprayed deposits and free-standing forms which varies with, among many variables, the plasma spraying process, spraying parameters, and the nature of the feedstock materials. Porosity influences the mechanical, electrical, thermal, and other properties of these deposits.¹

Porosity and porosity formation mechanisms for thermally sprayed deposits have not been extensively studied. Most studies have focused on the splat structure itself² and on the deposit microstructure.^{3,4} Theoretical studies of the porosity formation process introduce many simplifying assumptions,^{5,6} which may limit the usefulness of these approaches for practical porosity prediction.

The simplest model for pores in plasma sprayed deposits divides the pores into the subsystems of large pores and small pores.⁷ More elaborate porosity models⁸ are based on SEM studies of fracture surfaces. The models classify pores according to their morphology and divide them into more categories related to either size regimes or the probable formation process. The disadvantage of such models is that different pore types are not measured independently by quantitative techniques.

Various quantitative porosity techniques measure porosity; for example, mercury intrusion porosimetry (MIP), water immersion (sometimes called water displacement or the Archimedean method), and image analysis associated with optical microscopy or SEM. These techniques often yield different results for the same sample⁹ because different subsystems of pores are measured, e.g., open or closed pores, different size regimes.

In the present study, well characterized materials (alumina) are used to investigate very versatile and powerful porosity measurement technique, small-angle neutron scattering (SANS). This technique gives a new perspective on the pores in plasma sprayed deposits and

may enable more reliable modeling. The SANS technique is compared here with the MIP and water immersion measurements.

Background of the alumina material

In this research, alumina was chosen as a model material and heat treatment was selected as a typical processing step which alters porosity levels. Processes occurring during heat treatment of plasma sprayed alumina deposits have been studied^{10,11,12} in the past.

Plasma sprayed alumina passes through the set of phase transformations at $\sim 1200^{\circ}\text{C}$ from the original γ or δ phase to the final and stable α phase. This phase transformation results in an increase in density of about 10% (from 3.60 to 3.98 g/cm³) and therefore a decrease in the deposit bulk volume. This bulk densification manifests itself either as shrinkage of the sample or as an increase in the sample porosity. Porosity increase can proceed through growth of existing pores and through the creation of new porosity in the form of cracks.

Alumina sinters at temperatures greater than 1200°C , the sintering rate depending on the chemical composition of alumina. Some impurities, such as titania or iron, increase the sintering rate by 100 to 10000 times even when present at levels of less than 1 wt%.^{13,14} Sintering results in a porosity reduction and the growth of larger pores at the expense of smaller ones. This process reduces the total surface area of pores and, therefore, reduces the total surface energy of the pore system.

Experiments

Two alumina-based free-standing deposits were spray-fabricated from white and gray alumina (for particle size distribution and chemical compositions see Table 1). A water-stabilized plasma gun (PAL 160) at the Institute of Plasma Physics, Academy of Sciences of the Czech Republic, was used to spray the samples. This gun has an input power of 160 kW at an operating voltage of 320 V and current of 500 A. The spraying distance was approximately 300 mm. The powder feeding rate was about 20 kg/h using air as the carrier gas. The sprayed deposits were stripped from the 5 mm thick steel substrate to form deposits 2 to 3 millimeters thick. These deposits were studied in the as-sprayed state and after heat treating for 2 h at 1300°C or 1500°C .

The feedstock materials consisted mainly of the α phase. The white alumina (AB) also contained traces of β phase. Both materials were produced by fusing and crushing. After spraying, the samples consisted mainly of metastable γ and δ phases, with about 5 to 10 wt% of α phase. Both heat treatment temperatures resulted in transformation of the deposits into the α phase.

A mercury intrusion porosimeter, model Autoscan 33 (Quantachrom Corp., NY-USA), was used to study the

pores in the size region of 30 Å (0.003 μm) to 100 μm . Porosity, which can be accessed by intruded mercury, the apparent density (density including pores), and the residual density (density excluding pores) are measured by this method.

Water immersion porosimetry was used as the second method and yields data which may be defined in a fashion similar to MIP. However, the results may differ since MIP uses high pressures that may damage the sample structure and open pores that were originally closed.

The small-angle neutron scattering (SANS) method has been successfully applied to porosity studies of sintered alumina¹⁵ and other ceramic materials.^{16,17} Two different techniques of SANS were used in this study - Porod measurements and multiple small-angle neutron scattering (MSANS). These techniques enable the assessment of: (i) total surface area of all pores, (ii) volume-weighted effective pore radius (i.e., R_{eff}) of the pores in the size range 0.08 μm to 10 μm , and (iii) porosity volume in the same size range. The SANS measurements were performed at the Cold Neutron Research Facility at the National Institute of Standards and Technology (NIST) in Gaithersburg, Maryland, USA.

In the SANS experiment, Fig. 1, a beam of cold neutrons (wavelength of 5 to 18 Å) is passed through the sample. The neutrons are scattered at microstructural interfaces with different scattering length density; in the present study these scattering objects are the pores. The scattering angle depends on the wavelength and size of the pores. The larger the pore, the smaller the scattering angle.

The scattering curve of intensity vs. scattering angle can be divided into two regions. The multiple small-angle scattering region angles is dominated by neutrons scattered many times by large pores inside the sample. The theory of this multiple scattering (MSANS)^{18,19} is a useful tool for assessment of pores in the 0.08 to 10 μm range.²⁰ The volume-weighted effective pore radius (R_{eff}) and volume of porosity in the studied size region are the results of such measurements.

Larger scattering angles are dominated by scattering from the pores' surfaces in a region which is termed the "Porod region". The "internal" surface area of the pores can be determined with no theoretical assumptions of pore morphology or size.

Results and Discussion

Results of the intrusion techniques are presented in Table 2 and those of the SANS experiments in Table 3.

Volume of porosity

Three different techniques that were used to assess the volume of porosity, namely water immersion, MIP and SANS, are compared in the Fig. 2. The porosity measured by the water immersion technique was always smaller than

the MIP results; probably because water immersion measures open porosity at atmospheric pressures whereas MIP measures porosity opened at high pressures (3.300 psi; 22.8 MPa) used during the measurements. The MIP porosity is close or equal to the total porosity in the sample. This finding is supported by bulk densities measured by MIP, which are close to the densities of γ and α phases (for as-sprayed and samples heat treated 2 h at 1500°C, respectively).

The SANS and MIP results are similar for the heat treated samples within the margins of error, estimated to be ± 0.5 to 1.0 % for each technique. The SANS porosity was smaller than the MIP porosity for as-sprayed samples. This suggests a change in the porosity characteristics upon heat treatment. The likely reason is that part of the porosity in the as-sprayed samples is smaller than the size region measured by the MSANS technique, i.e., it is smaller than 0.08 μm . These pores increase in size on heat treatment and therefore become included in the measured MSANS region. The process of the pore size increase can be related to the phase transformation sequence of $\gamma \rightarrow \delta \rightarrow \alpha$.

Pore characteristics

The MSANS studies allowed R_{eff} to be measured. In the present study R_{eff} is equal to the volume weighted radius of the spheres.

The R_{eff} changed for the AB and AH materials with heat treatment, Fig. 3, depending on chemistry. The R_{eff} for AB material shrank under the 1300°C/2 h heat treatment and then stayed the same. The R_{eff} for AH material stayed the same under the 1300°C/2 h heat treatment and then grew for the 1500°C/2 h heat treatment. Values of R_{eff} are between 0.6 and 1.0 μm for all samples with the exception of the AH sample, heat treated 2 h at 1500°C, for which R_{eff} reached 2.2 μm . The estimated error of these measurements is ± 0.1 μm .

The decrease of R_{eff} during the first heat treatment agrees with the porosity volume results. A reduction in R_{eff} may arise due to an increase of the number of small pores counted in the measuring process. This increase may be caused by a size increase of pores already in the sample during the phase transformation.

The size increase at the 1500°C/2 h heat treatment for gray alumina is significantly larger than for white alumina and can be explained by the higher sintering rate for the gray alumina at this temperature.

Surface (Porod) measurements show the same tendency for both samples, Fig. 4. Pore surface area for the as-sprayed condition increased (2.5 to 3.2×10^4 cm^2/cm^3) to about 3 times (7.1 to 7.6×10^4 cm^2/cm^3) for the 1300°C/2 h heat treatment and then decreased. An increase during the first heat treatment can be related to crack formation during the phase transformation $\gamma \rightarrow \delta \rightarrow \alpha$. The fact that the as-sprayed and 1300°C/2 h heat treated

samples exhibited similar surface areas suggests that the processes of surface formation are also similar. At 1500°C/2 h heat treatment, the surface areas differ by more than 3 times and there are probably large differences in the processes at this temperature. A likely explanation is the difference in the sintering rate, which, for gray alumina, is significantly higher than for white alumina.^{10,11} A higher sintering rate results in the elimination of small pores and in an increase of the large ones, as discussed previously.

Conclusions

1. Small-angle neutron scattering is a valuable tool in studies of porosity in ceramic plasma sprayed deposits. It non-destructively measures the porosity and pore characteristics that are inaccessible with other techniques or which measurements are limited by model requirements.
2. The measurement arising from mercury intrusion porosimetry is close to the total porosity as manifested by the measured bulk densities. The water immersion method measured 50 to 90% of the MIP measured porosity.
3. The small-angle neutron scattering yielded porosities which were close to the MIP measurements of heat treated samples and smaller than MIP in as-sprayed samples. This suggests that part of the porosity in the as-sprayed samples is below the measurable size range of the MSANS technique, i.e., smaller than 0.08 μm .
4. The volume weighted pore effective radii (R_{eff}) measured in the size range of 0.08 to 10 μm were about 0.6 to 0.8 μm for as-sprayed alumina deposits and changed with the heat treatment.
5. The pore size distribution in deposits changed when the materials were heat treated for 2 h at 1300°C. This change manifests itself in a decrease of R_{eff} and an increase of the porosity detected by MSANS. A possible explanation of this fact is an increase of sizes of existing pores and possible formation of new pores, so the number of pores with sizes around 0.1 μm increases.
6. Processes in the deposits differ on heat treatment for 2 h at 1500°C and result in changes in R_{eff} . For white alumina (AB) under these conditions R_{eff} does not change significantly. For gray alumina with a sintering rate at least 100 times larger, R_{eff} increases by about 3 times.
7. Small-angle neutron scattering also allows determination of the surface area of the pores in the deposits. These internal surfaces are about 3×10^4 cm^2/cm^3 for as-sprayed deposits.
8. Pore surfaces increase significantly (more than double) with heat treatment for 2 h at 1300°C and decrease for 2 h at 1500°C.

References

1. Taylor R., Brandon J. R., and Morell P., Microstructure, Composition and Property Relationships of Plasma Sprayed Thermal Barrier Coatings, *Surf. and Coat. Tech.*, 50, (1992) 141-149.
2. Wilms V. H. S., The Microstructure of Plasma Sprayed Ceramic Coatings, Ph.D. Thesis, SUNY at Stony Brook, New York, 1978, (UnM) AA17819123.
3. Pawlowski L., Microstructural Study of Plasma-Sprayed Alumina and Nickel Chromium Coatings, *Surf. and Coat. Tech.*, 31, (1987) 103-116.
4. Shi Ke-Shun, Qian Z-Y., Zhuang M-S., Microstructure and Properties of Plasma Sprayed Coating, *J. Am. Ceram. Soc.*, 71 [11], (1988) 924-929.
5. Fukanuma H., An Analysis of the Porosity Producing Mechanism, pp. 767-772 of *Thermal Spray: International Advances in Coatings Technology*, Ed: C. C. Berndt, Pub. ASM Int., Materials Park, OH, USA, 1992.
6. Pekshev P. Yu. and Murzin I. G., Modeling of Porosity of Plasma Sprayed Materials, *Surf. and Coat. Tech.*, 56, (1993) 199-208.
7. Uematsu S., Amada S., Senda T., and Sato S., On Pore Structure of Plasma-Sprayed Films, pp. 379-383 of *Proceedings Int. Symp. on Advanced Thermal Spraying Technologies and Allied Coatings*, Pub. High Temp. Soc. of Japan, Osaka, Japan, 1987.
8. Pekshev P. Yu. and Safiullin V. A., Porosity of Plasma Sprayed Alumina, pp. 437-462 of *High Temperature Dust-Laden Jets in Plasma Technology*, Eds: O.P. Solonenko, A.I. Fedorchenco, Pub. VSP, Utrecht, The Netherlands, 1990.
9. Ilavsky J., Berndt C. C., Herman H., Forman J., Dubsky J., Chraska P., and Neufuss K., Analysis of Porosity of Free-Standing Ceramics Manufactured by Plasma Spraying, pp. 505-512 of *Thermal Spray Coatings: Research, Design and Applications*, Ed: C. C. Berndt and T. F. Bernecki, Pub. ASM Int., Materials Park, OH, USA, 1993.
10. Bagley R. D., Cuttler I. B., and Johnson D. L., Effect of TiO_2 on Initial Sintering of Al_2O_3 , *J. Am. Ceram. Soc.*, 53 [3], (1970) 136-141.
11. Brook R. J., Effect of TiO_2 on Initial Sintering of Al_2O_3 , *Journal of American Ceramic Society*, 55 [2], (1972) 114-115.
12. Heintze G. N. and Uematsu S., Preparation and Structure of Plasma Sprayed γ - and α - Al_2O_3 Coatings, *Surf. and Coat. Tech.*, 50, (1992) 213-222.
13. Iwamoto N., Makino Y., and Arata Y., Crystallographical Considerations on Sprayed Alumina, pp. 190-196 of *General Aspect of Thermal Spraying*, Proceedings of 9th International Spraying Conference, Pub. Nederlands Instituut voor Lastechniek, The Hague, Nederlands, 1980.
14. Thompson V. S. and Whittemore O. J., Structural Changes on Reheating Plasma-Sprayed Alumina, *Am. Cer. Soc. Bull.*, 47 [7], (1968) 637-641.
15. Hardman-Rhyne K. A. and Berk N. F., Small-Angle Neutron Scattering from Porosity in Sintered Alumina, *J. Am. Ceram. Soc.*, 69 [11], (1986) C285-287.
16. Hardman-Rhyne K. A. and Berk N. F., Characterization of Alumina Powder Using Multiple Small-Angle Neutron Scattering II. Experiment, *J. Appl. Cryst.*, 18, (1985) 473-479.
17. Long G. G., Krueger S., Gerhardt R. A., and Page R. A., Small-Angle Neutron Scattering Characterization of Processing/Microstructure Relationships in the Sintering of Crystalline and Glassy Ceramics, *J. Mater. Res.*, 6 [12], (1991) 2706-2715.
18. Hardman-Rhyne K. A., Frase K. G., and Berk N. F., Application of Multiple Small Angle Neutron Scattering to Studies of Ceramic Processing, *Physica*, 136B, (1986) 223-225.
19. Berk N. F. and Hardman-Rhyne K. A., The Phase Shift and Multiple Scattering in Small Angle Neutron Scattering: Application to Beam Broadening From Ceramic, *Physica*, 136B, (1986) 218-222.
20. Berk N. F. and Hardman-Rhyne K. A., Characterization of Alumina Powder Using Multiple Small-Angle Neutron Scattering I. Theory, *J. Appl. Cryst.*, 18, (1985) 467-472.

Acknowledgments

The authors thank co-workers from the Institute of Plasma Physics (Prague, The Czech Republic), namely, Mr. K. Neufuss and Mr. J. Dubsky, for their skill in sample preparation. This work has been partially supported under the NSF STRATMAN program (DDM 9215846). The use of the neutron facilities at NIST is gratefully acknowledged. One of the authors (A.N.G.) gratefully acknowledges financial support from the Department of Applied Science, Brookhaven National Laboratory (US Department of Energy Contract No. DE-AC02-76CH00016).

Table 1. Feedstock materials used in this study.

Sample	Chemistry	Particle sizes
AB (white alumina)	0.1% Fe <0.1% Ca <0.1% Cu	40 - 80 μ m
AH (gray alumina)	4.7% TiO_2 0.9% Fe	50 - 63 μ m

Table 2. Results of the intrusion techniques.

Sample	Water immersion		Mercury intrusion		
	Porosity [vol. %]	Apparent density [g/cm ³]	Porosity [vol. %]	Apparent density [g/cm ³]	Bulk density [g/cm ³]
AB - as-sprayed	5.9	3.32	11.1	NA	NA
AB - 2h at 1300°C	8.9	3.43	10.8	3.47	3.84
AB - 2h at 1500°C	9.1	3.48	10.4	3.62	4.02
AH - as-sprayed	5.3	3.37	7.4	3.43	3.71
AH - 2h at 1300°C	5.0	3.49	7.9	3.56	3.81
AH - 2h at 1500°C	5.3	3.52	7.9	3.68	3.91

Table 3. Results of the image analysis and SANS experiments.

SAMPLE	Porod Surface x10 ⁴ [cm ² /cm ³]	MSANS Porosity [vol %]	MSANS Effective Particle Radius (R _{eff}) [μm]
AB- As-sprayed	2.5	8.2	0.95
AB - 2h for 1300°C	7.1	11.2	0.63
AB - 2h for 1500°C	5.3	9.9	0.67
AH - As-sprayed	3.2	6.8	0.79
AH - 2h for 1300°C	7.6	8.0	0.77
AH - 2h for 1500°C	1.5	7.9	2.20

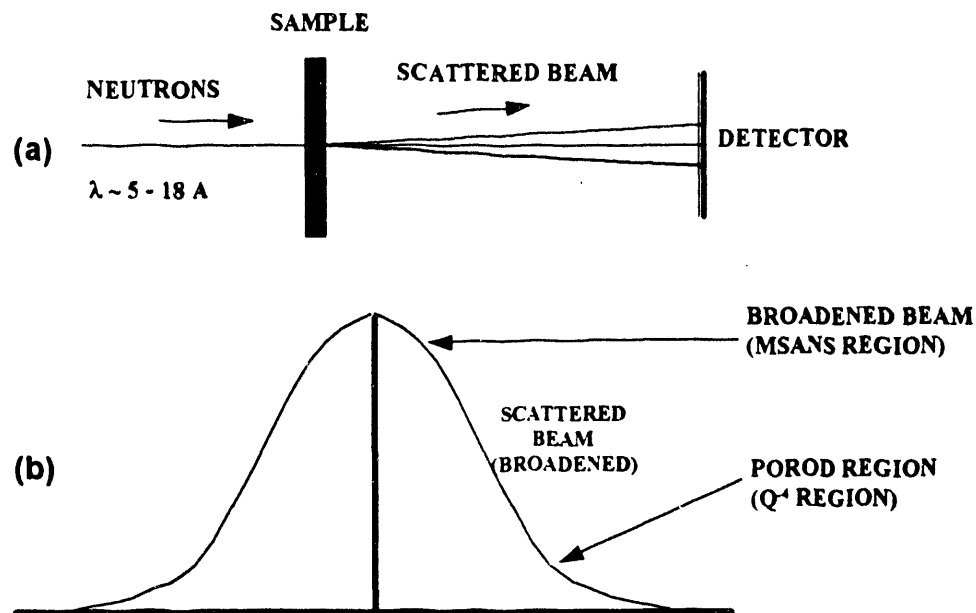


Figure 1. Schematics of the small angle neutron scattering (SANS). Part (a) shows the experimental arrangement and part (b) depicts the detector response.

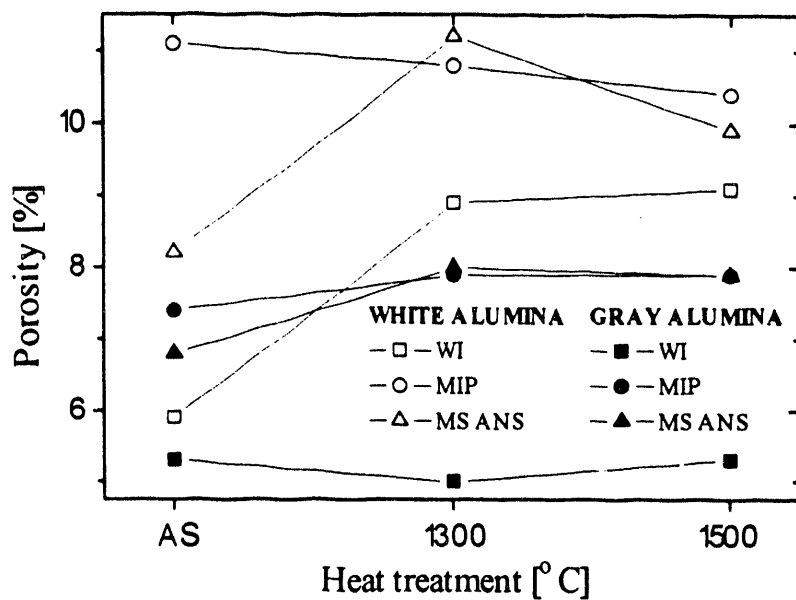


Figure 2. Porosity measured by different techniques (AS denotes as-sprayed sample, 1300°C denotes sample heat treated 2h at 1300°C and 1500°C denotes sample heat treated 2h at 1500°C).

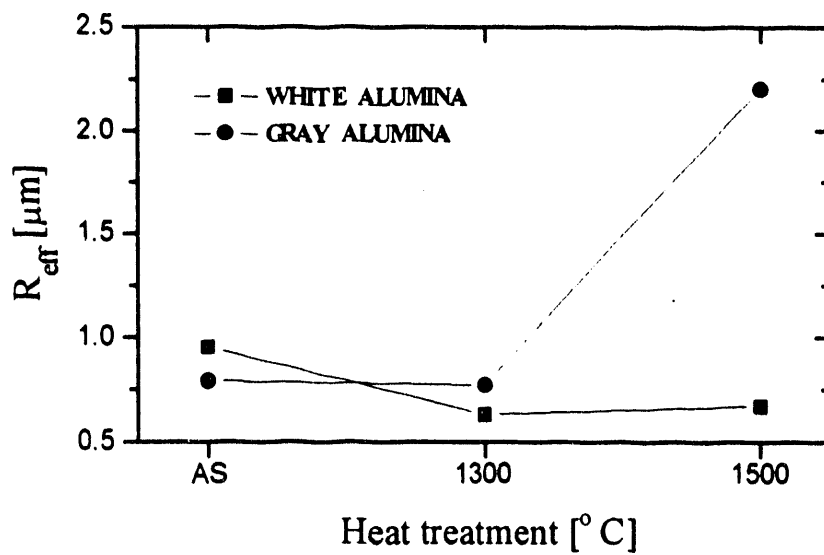


Figure 3. R_{eff} of the pores measured by MSANS technique (AS denotes as-sprayed sample, 1300°C denotes sample heat treated 2h at 1300°C and 1500°C denotes sample heat treated 2h at 1500°C).

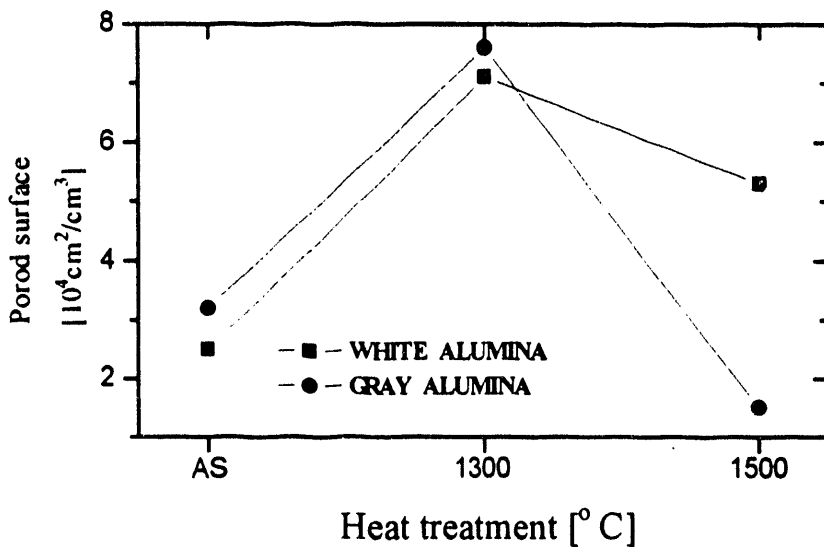


Figure 4. Pore surface as measured by SANS measurement (AS denotes as-sprayed sample, 1300°C denotes sample heat treated 2h at 1300°C and 1500°C denotes sample heat treated 2h at 1500°C).

The image is a high-contrast, black-and-white graphic. It features three horizontal bands. The top band is composed of three vertical rectangles of different widths, with the central one being the widest. The middle band is a single, thick, horizontal rectangle. The bottom band is also a single, thick, horizontal rectangle, but it contains a small, dark, irregular shape on its right side, possibly a hole or a tear.

DATA
MANAGEMENT

